Systematic Design and Optimization Method of Multimode Hybrid Electric Vehicles Based on Equivalent Tree Graph

Tao Deng, Peng Tang, Zhenghua Su, and Yuanping Luo

***Abstract*—Multimode hybrid electric vehicles (HEVs) have been widely applied due to its high efficiency and excellent overall performance. However, the introduction of multimode HEVs makes it difficult to choose reasonable design factors (architectures, component parameters, and control strategies) and determine correct mode shift rules, which undoubtedly enhances design complexity. To improve the design efficiency and reduce screen difficulty of optimal multimode configurations, a systematic design method is proposed to generate, screen, and optimize multimode HEVs with a single planetary gear. Based on equivalent tree graph method, the novel architectures are first generated. Then, considering mode shift rules and component parameters, requirements of speed and torque in corresponding main mode and minimum shift rule graph of working modes are taken as constraints to complete configuration screening. Finally, the equivalent consumption minimization strategy considering the proposed mode shift rules is put forward to evaluate and optimize energy management. The numerical results show that fuel economy of optimized configurations is improved by at least 22.1%, which proves the effectiveness of proposed systematic design method. Furthermore, it reveals that the multimode configuration can achieve better fuel economy when adopting the appropriate mode shift rule and designing the right arrangement and number of clutches and brakes.**

***Index Terms*—Equivalent consumption minimum strategy (ECMS), equivalent tree graph, hybrid electric vehicles (HEVs), mode shift rule, multimode.**

I. Introduction

HYBRID electric vehicles (HEVs) have outstanding energy conservation potential and powerful operation control ability, which is one of the schemes that can effectively alleviate energy shortage and environmental pollution [1]–[3]. The energy conservation potential of HEV mainly depends on the component parameters, mechanical connection between components, and instantaneous power distribution rule between power sources, that is, configuration and energy management [4], [5]. Configuration is the basis of energy management, which determines algorithm selection, optimization potential, operation mode, and power allocation strategy of HEV, and directly affects automobile dynamic performance and fuel economy (FE) [5], [6].

According to the configuration type, the HEVs are generally classified into four categories: series, parallel, power-split, and multimode. At present, the power-split HEVs occupy the mainstream market, which can also be subdivided into single planetary gear (PG), double-PG, and multi-PG power-split configurations. The engine and motors of power-split configurations are coupled by the PG to achieve continuously variable transmission, such as Toyota hybrid system I (THS-I) [7], [8], THS II [8], [9], and extended configurations [10], [11].

Due to the few operation modes for the power-split HEVs, it is difficult to balance the FE of urban and high-speed working condition. Thus, the multimode HEVs were proposed to solve this dilemma via adding clutches and brakes on the power-split HEVs [12], [13]. For example, the multimode transmission for an HEV with two-PG, two clutches, and two brakes can achieve 16 modes [14]. And its fuel efficiency is better than THS-II system. However, due to lack of systematic design methods, it is difficult to generate a large number of novel multimode HEVs.

Thus, it is significant to propose a systematic design and optimization method to further explore mechanism potential and generation efficiency for multimode HEVs. At present, the most popular design methods mainly include lever method [15], [16], graph theory [17], dynamic matrix (D-matrix) [18], and so on. On the basis of lever method, the authors in [19] and [20] proposed a four-node compound lever method and a compound allocation configuration method of power-split system with lever reverse resolution, respectively, which improved computational efficiency and application range. However, lever method cannot be applied to analyze and screen a large number of configurations because its kinematics equations need to be extracted manually. Graph theory can simplify the complex study object into points and lines and express the connection relation of each component through the adjacency matrix. Pei *et al*. [21] utilized hierarchical topological graph to analyze and redesign THS-I system and proposed more feasible configurations. But they

Manuscript received December 9, 2019; revised February 23, 2020; accepted April 18, 2020. Date of publication April 26, 2020; date of current version July 31, 2020. Recommended for publication by Associate Editor M. Ferdowsi. This work was supported in part by the National Natural Science Foundation of China under Grant 51305473, in part by the Scientific and Technology Research Program of Chongqing Municipal Education Commission under Grant KJQN201800718, and in part by the Fifth Group Project Supported by Outstanding Talents of Institutions of Higher Education in Chongqing. *(Corresponding author: Tao Deng.)*

Tao Deng is with the School of Aeronautics, and also with School of Mechatronics & Vehicle Engineering, Chongqing Jiaotong University, Chongqing 400074, China (e-mail: d82t722@cqjtu.edu.cn).

Peng Tang, Zhenghua Su, and Yuanping Luo are with the School of Mechatronics & Vehicle Engineering, Chongqing Jiaotong University, Chongqing 400074, China (e-mail: 1006326195@qq.com; 631387041@qq.com; 473777243@qq.com).

Color versions of one or more of the figures in this article are available online at https://ieeexplore.ieee.org.

Digital Object Identifier 10.1109/TPEL.2020.2990209

ignored the influence of clutch and brake on configuration design. Nevertheless, graph theory also needs to manually extract dynamic equation; so its computational complexity is still high. Liu and Peng [18] first proposed D-matrix method to generate single-mode HEV. Zhang *et al*. [12], [22]–[24] further optimized this method and realized the automatic generation of multimode configuration from a single-PG to three-PG when considering the increase and decrease of clutches. However, this optimized D-matrix method ignored configuration generation when power source was connected internally. For example, engine and motor were mutually connected and connected together on the same node of PG.

The core of the above three methods is to simplify the configuration and extract its main characteristics or dynamic equations. In addition, many scholars explored the optimal configurations through efficiency analysis of current HEVs or relevant performance evaluation. For example, Zhou *et al*. [25] proposed the optimal selection method by optimizing and comprehensively evaluating the design scheme of HEV powertrain. Hu *et al*. [6] provided a new configuration design method though efficiency optimization of the whole powertrain.

Although the design method of multimode HEVs has made great progress, it still depends on engineering experience of designers or functional expansion on the basis of existing configurations and fails to propose systematic design method. Moreover, when the mode shift rules and design factors (architectures, component parameters, and control strategies) are not reasonable, the phenomenon of power flow backflow and disorder will occur, which will lead to low energy utilization rate. Therefore, it is necessary to explore the influence of mode shift rules and design factors on the original innovative design of HEVs. The design method solely based on existing experience is bound to bring limitations on configuration systematic design. In this study, a systematical design method is proposed to generate, screen, and optimize the multimode HEVs with a single PG, which fully considers the architectures, component parameters, and mode shift rules. Furthermore, equivalent consumption minimum strategy (ECMS) combined with optimal mode shift rule is put forward to verify the effectiveness of proposed method.

There are three main novelties in our research. One is that the adopted configuration generated method based on equivalent tree graph is original and totally different with the existing method. Another is that the minimum shift rule graph of working modes utilized to screen the HEVs is more effective when considering the orderly energy flow conversion. And the third one is that the control strategy ECMS considering the optimal mode shift rule can enhance the energy utilization rate for HEVs significantly.

The rest of this article is organized as follows. The equivalent tree graph method is proposed in Section II. Section III presents the generation process of single-mode and multimode HEVs. The multimode HEVs are analyzed and screened through dynamic constraints and minimum shift rule graph of working modes in Section IV. ECMS considering mode shift rules is presented in Section V. And, the proposed multimode HEVs are further optimized in Section VI. Finally, the conclusion is presented in Section VII.

TABLE I
EQUIVALENT TREE GRAPH MODEL SYMBOLOGY

Symbol	Representation of components	Corresponding tree element
	Connection between PG	Trunk
	Connection between planetary gears and input/output source	Branch
	Brake	Leaf
	Clutch	
	Input or output power source	Node
	Planetary gears	

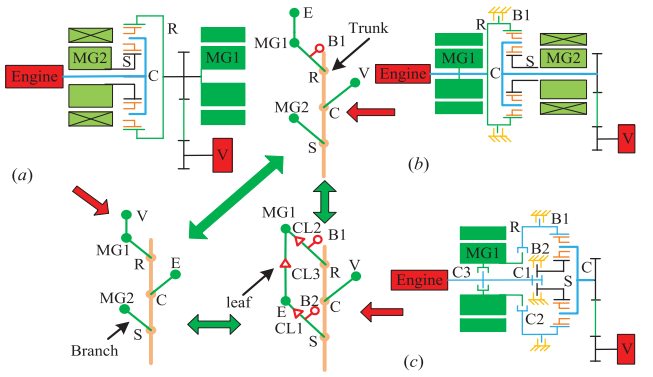

Fig. 1. Powertrain architectures and corresponding equivalent tree graphs.

II. EQUIVALENT TREE GRAPH METHOD

When a graph model of HEV is used to describe configuration topology relationships, it is necessary to carry building information, logical information, hierarchical information, and isomorphism information [21]. Because there is obvious logical and hierarchical relation in the tree, an equivalent tree graph method is proposed to better describe the hybrid powertrain. In equivalent tree graphs, the elements of HEV powertrain are shown by nodes, such as engine (*E*), motor (MG1), generator (MG2), output shaft to vehicle wheel (*V*), sun gears (*S*), ring gear (*R*), and carrier (*C*). And, the relationships between those elements are expressed by lines, as shown in Table I.

According to Table I, the powertrains of Toyota Prius [7], [8], the Chevy Volt [26], and those proposed by Ehsani *et al*. [27] are modeled as equivalent tree graphs, as shown in Fig. 1.

The PG, power source, and their interconnection with other nodes and brakes or clutches can be represented by the trunk, branch, and leaf of the tree in Fig. 1. Thus, the new trees can be generated via random combinations of different trunks, branches, and leafs. However, it is not easy to effectively generate the reasonable trees due to its high randomness and calculation burden. To improve the efficiency and quality of generation, the combination process is limited to a random combination of branch and several specific branches with leafs. Through current configurations, a tree library including almost all kinds of branches and trunk is produced, as shown in Fig. 2.

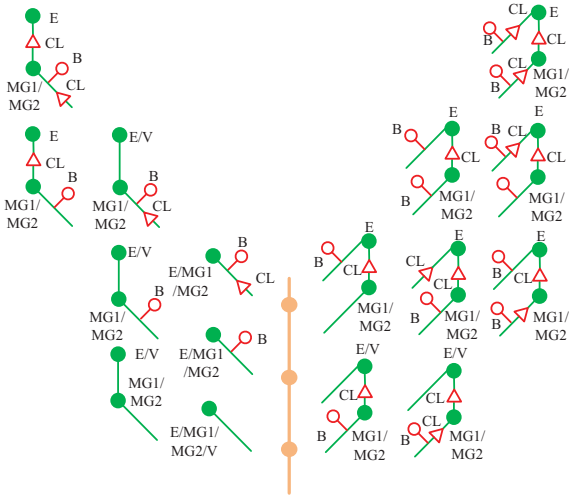

Fig. 2. Tree library with trunk and different branches.

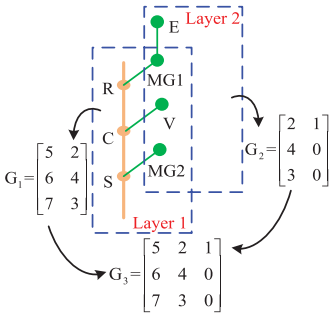

Fig. 3. Two-layer connection diagram of a single-mode HEV.

III. Generation Process of Trees

A. The Generation Process of Trees Without Leafs

By analyzing the above tree library, there are two connection relations, namely the internal connection of power sources and the connection between each power source and PG. To better describe these two connection relations, a two-layer connection diagram of a single-mode HEV is adopted as shown in Fig. 3.

In Fig. 3, layer 1 indicates the connection between power sources (MG1, MG2, and *V*) and PG, while layer 2 displays the connection between MG1 and *E*. And the connection of these two layers can be expressed with matrix G1 and G2. Among the matrixes, *E*, MG1, MG2, *V*, *R*, *C*, and *S* are coded to be "1," "2," ..., "7," respectively. And, the matrix G3 of the corresponding tree can be generated by means of G1 and G2. To simplify the generation process of G3, its first column is always set to be [5, 6, 7]. Thus, G3 can be expressed by G2. That means the generation process of trees without leafs is to obtain the matrix G2 through random combination of any two power source vectors.

Assuming the number *N* of tree is 4, the specific generation can be expressed, as illustrated in Fig. 4.

In order to realize the unique expression of power source vector, weight *S* is formulated as follows:

$$\begin{cases} S(x) = h_1 w^2 + h_2 w + h_3 \\ h_1 = \min(a,b,c), h_3 = \max(a,b,c) \\ h_2 = a + b + c - h_1 - h_3 \end{cases} \tag{1}$$

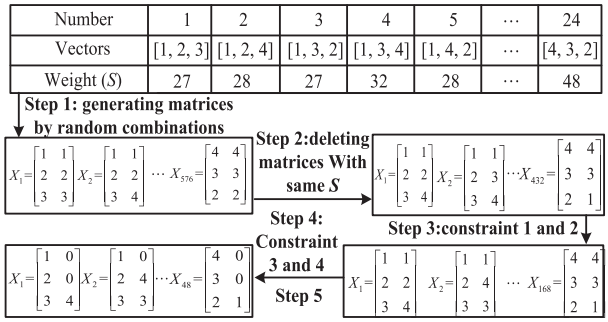

Fig. 4. Generation process of trees without leafs when *N* is 4.

TABLE II
Main Constraints

Constraints	Rules
Constraint 1	E cannot be directly connected to V, and MG1 cannot be directly connected to MG2.
Constraint 2	MG1 or MG2 cannot be simultaneously connected to another MG2 or MG1, V, and one node of PG.
Constraint 3	The power source cannot be simultaneously connected to all three nodes of PG.
Constraint 4	E/V cannot be directly connected to other two power sources and one PG node simultaneously.

where *w* is the number of power source, *a*, *b*, and *c* denote the codes of three corresponding components, respectively, h_1 and h_3 are the minimum and maximum values of *a*, *b*, and *c*, respectively, and h_2 is the value between h_1 and h_3. In step 5, if two elements of a row vector are exactly the same, the corresponding parts of second column elements are represented by 0. And, constraints 1–4 in the above steps are shown in Table II. Through generating and screening trees in Fig. 4, 48 configurations with four power sources and a single PG are obtained.

B. The Generation Process of Trees With Leafs

Multimode HEV requires brakes and clutches to control the switching of different working modes. Thus, novel trees can be created by adding leafs in the above trees. Through analyzing features of the obtained 48 kinds of trees, they can be divided into next four tree topologies. Meanwhile, one of the four topologies is selected as study object, and the generation process of trees with leafs is shown in Fig. 5.

In Fig. 5, brake and clutch are coded to be "8" and "9," respectively. In step 3, vector [5, 8] means that brake is fixed on node *R*. And, vector [1, 2] means that clutch is fixed between E and MG1. Step 4 is used to synthesize vector matrices with different numbers of clutches and brakes. And the number can be expressed with *k*. According to number of brakes and clutches on branches in Fig. 2, the maximum value of *k* is determined. Thus, 123 matrixes are finally obtained, which describe the connection relation among nodes, brakes, and clutches. In step 6, the matrix of brakes and clutches is combined with tree matrix. And the new matrix can be obtained and backtracked to corresponding tree graph. For example, the new tree can be obtained with M_{48} and $L_1{}^*$, as shown in Fig. 6.

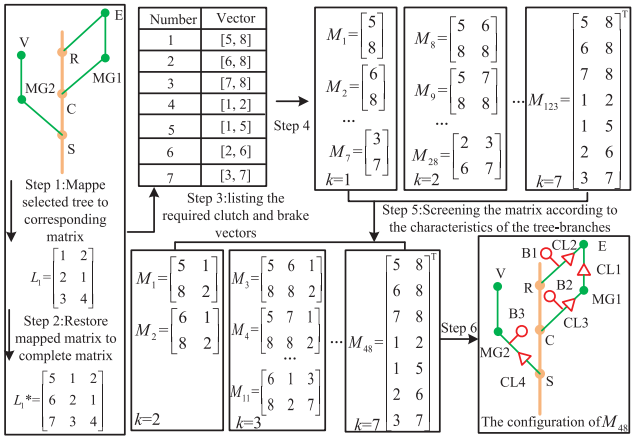

Fig. 5. Generation process of trees with leafs.

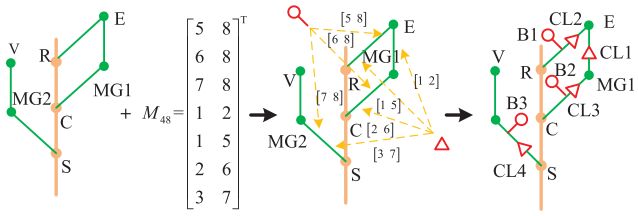

Fig. 6. Combination process of the selected tree and M_{48}.

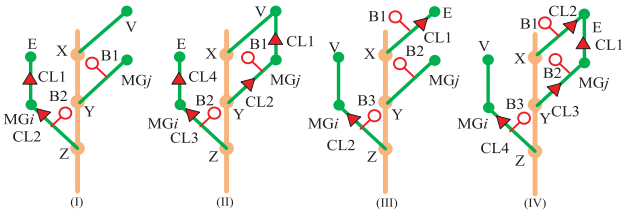

Fig. 7. Four novel trees.

And four types of corresponding trees with the maximum number of leafs according to the above generation process are illustrated in Fig. 7. Note that *R*, *C*, and *S* are expressed by any one of *X*, *Y*, and *Z*, respectively. And all of *X*, *Y*, and *Z* are not equal. In summary, 2304 configurations of multimode HEVs with a single PG can be obtained totally.

IV. Trees Screening

A. Establishment of Mode Shift Rule

The tree in Fig. 7(I) is selected as an example to analyze its rationality. In view of different states of clutch and brake, 12 working modes are obtained. The corresponding power flows are displayed, as shown in Fig. 8. It should be noted that the symbol "▲" or "●" denotes locked phase of clutch of brake, and symbol "→" indicates power flow.

As the type and number of working modes increase, the optimal FE can be achieved. However, the formulation of mode shift rules will become more complex. Thus, the mode shift rules should be considered when generating the trees. Due to the limited response time of clutch and brake, no more than

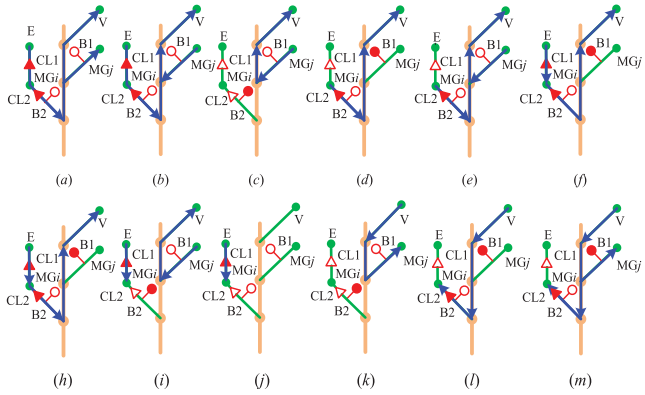

Fig. 8. Power flow diagram of 12 modes.

TABLE III
Mode Shift Rules Definition

Rules	Definition
1	It contains at least 8 major modes
2	Each mode can be directly switched to regenerative braking mode
3	Pure electric mode can be switched to any other modes
4	EVT/power-split/parallel/ engine alone /series mode can be directly switched to any other modes except parking charging mode

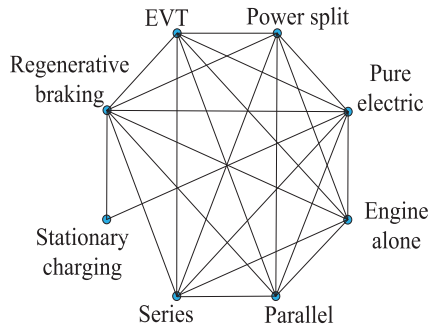

Fig. 9. Minimum shift rule graph of working modes.

two components can operate at the same time during different working mode switching [14]. To formulate appropriate mode shift rules, the above 12 working modes are analyzed. In order to enhance the utilization of working modes and eliminate the backflow and disorder of power flow, the mode shift rules are defined through the existing energy management strategies and common working modes of related configurations, as demonstrated in Table III.

Meanwhile, in order to facilitate analysis and further screening, a minimum shift rule graph of working modes is formulated based on the mode shift rules in Table III, as shown in Fig. 9.

B. Trees Screening Considering Mode Shift Rule

For multimode HEV, the type and number of working modes are determined after completing design work. Since HEV can achieve better performance with reasonable mode shift rule, the minimum shift rule graph of working modes is taken to judge

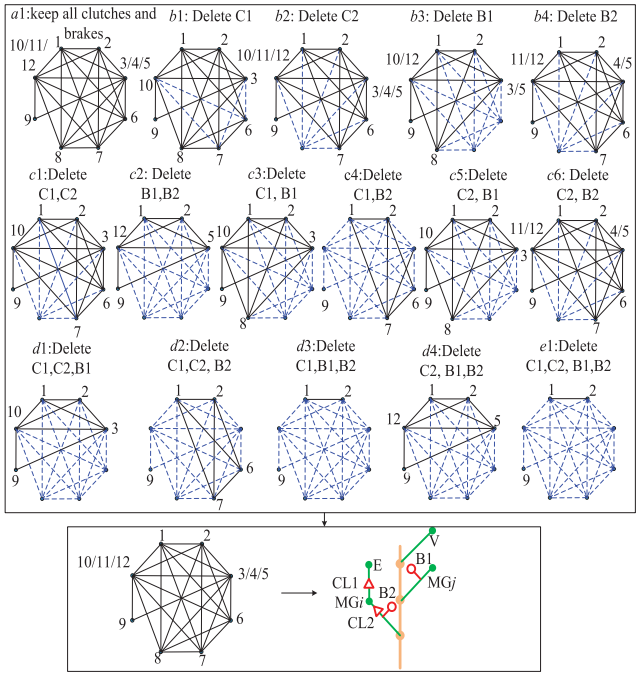

Fig. 10. Effective tree discrimination process.

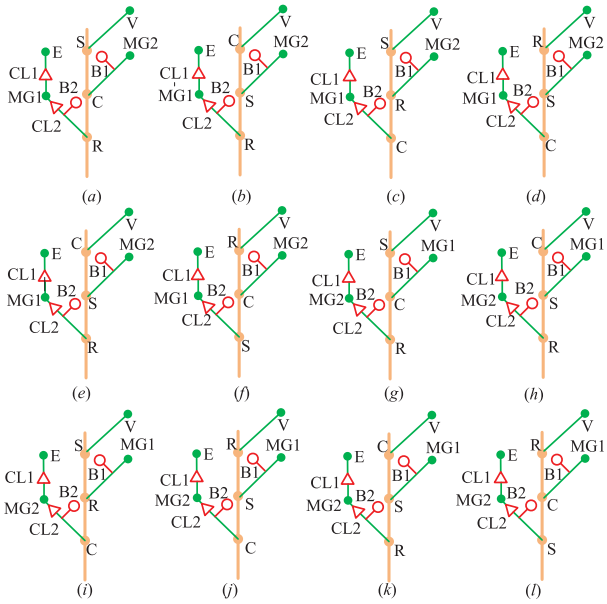

Fig. 11. Twelve new trees.

whether the tree is reasonable so as to complete further screening. The selected tree in Fig. 7(I) has seven leafs. According to the tree library in Fig. 2, the minimum value of leafs in this tree is zero. Thus, other trees can be obtained by removing the leaf one by one and screened by minimum shift rule graph. The effective tree discrimination process with different numbers of leafs is shown in Fig. 10.

The blue dotted line means the two modes cannot be switched. But, the black solid line means the two modes can be switched. After discriminating 16 trees included in the selected tree, it is found that only tree "*a*1" meets the requirements. So the other trees can be screened out. Then 12 new trees can be obtained after the location of PG, MG1, and MG2 is determined, as illustrated in Fig. 11.

C. Trees Screening Considering Valid Working Modes

The proposed multimode HEV should at least have engine alone driving, parallel driving, power-split mode, and so on. So the rotational speed and torque relationship under these modes can be first analyzed to determine whether it meets the requirements. In this article, all the models of main components are selected from Advisor 2002, and the system parameters are shown in Table IV.

According to the efficiency maps and the speed and torque range of engine, MG1, and MG2, the application rationality of several modes are discussed. For power-split mode, the driving motor is coaxially connected to the engine. And motor and engine together provide the required torque. Then, the combined output torque is converted into the driving torque in front of the final gear and compared with the maximum required torque in front of the final gear, as shown in Fig. 12(a). Similarly, the comparison between the main driving torque of the other

TABLE IV
VEHICLE PARAMETERS

System	Parameters	Values
Vehicle	Gross mass	1360 kg
	Windward area	1.746 m^2
	Aerodynamic drag factor	0.3
	Wheel radius	0.287 m
	Rolling resistance coefficient	0.009
Final drive	Gear Ratio	3.93
PG	Ring/Sun Gear ration	2.6
Battery	Capacity	30 Ah

remaining five modes and the required torque in front of the final gear can be analyzed one by one, as shown in Fig. 12(b)–(f).

Fig. 12(e) and (f) shows that configurations (1), (3), (6), (7), and (9) do not meet torque requirement in parallel driving mode. While configurations (7), (9), (10), (11), and (12) do not meet torque requirement in series driving mode. Since the torque of engine and MG1 are the same in series driving mode, it is impossible to force both engine and MG1 to run within high efficiency operating range. However, MG2 can replace MG1 to meet the charging demand in series driving mode because its high-efficiency generation interval coincides with the high-efficiency operation interval of engine. Therefore, configurations (1)–(6) can be excluded. Meanwhile, the remaining configuration (8) can be verified according to both speed and torque relationship. And it still meets the requirements of both speed and torque. Thus, tree (8) in Fig. 11 is adopted as our study object.

V. DETERMINATION AND ANALYSIS OF CONTROL STRATEGY

A. Determination of ECMS Considering Mode Shift Rule

Derived from Pontryagin's minimum principle [28], [29], ECMS is adopted as the control strategy in this article. As an

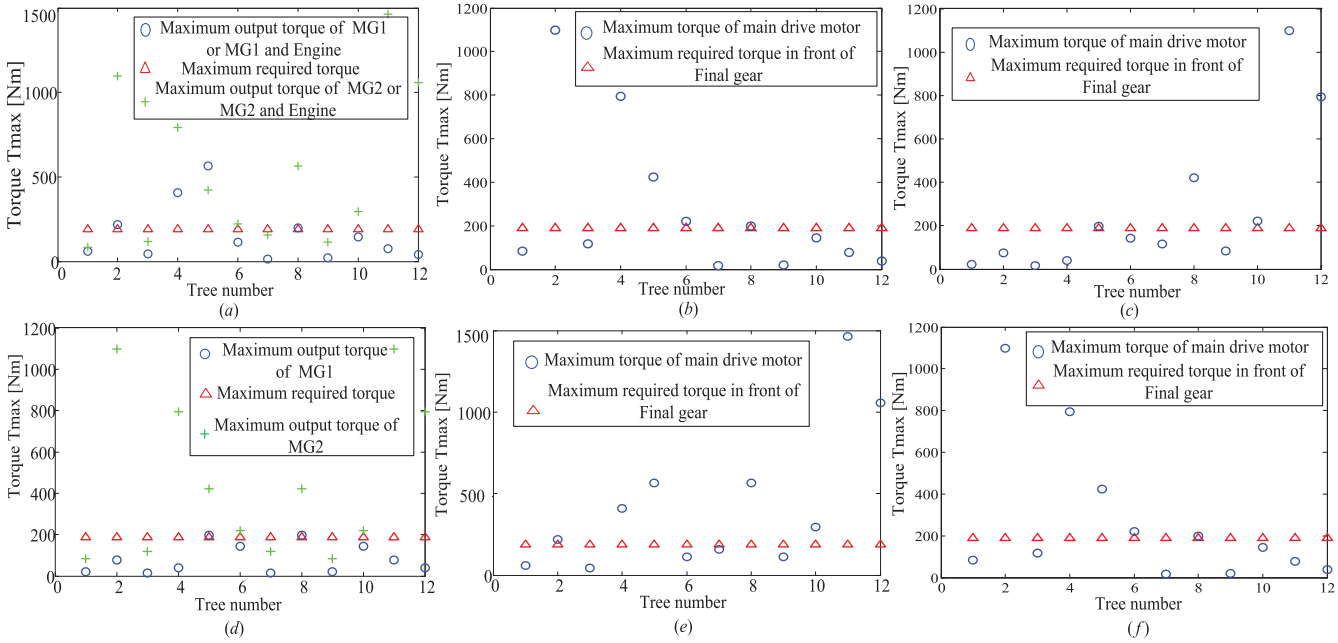

Fig. 12. Comparisons between different main drive torques and required torques under several modes.

instantaneous optimization strategy, the objective function of ECMS is expressed as follows:

$$m_{\mathrm{eqv}}(\omega_{\mathrm{e}}(t), T_{\mathrm{MG}i}(t), s(t), t) = m_{\mathrm{e}}(\omega_{\mathrm{e}}(t), T_{\mathrm{MG}i}(t), t) + s(t)\frac{P_{\mathrm{bat}}(\omega_{\mathrm{e}}(t), T_{\mathrm{MG}i}(t), t)}{Q_{\mathrm{LHV}}} \tag{2}$$

$$\text{Subject to} \begin{cases} T_{e\_\min} \le T_e \le T_{e\_\max} \\ \omega_{e\_\min} \le \omega_e \le \omega_{e\_\max} \\ T_{\mathrm{MG}i\_\min} \le T_{\mathrm{MG}i} \le T_{\mathrm{MG}i\_\max} \\ \omega_{\mathrm{MG}i\_\min} \le \omega_{\mathrm{MG}i} \le \omega_{\mathrm{MG}i\_\max} \\ SOC_{\min} \le SOC \le SOC_{\max} \\ I_{\mathrm{bat\_min}} \le I_{\mathrm{bat}} \le I_{\mathrm{bat\_max}} \\ P_{\mathrm{bat\_min}} \le P_{\mathrm{bat}} \le P_{\mathrm{bat\_max}} \\ \mathrm{Mode} \in \{1, 2, 3, \ldots, 12\}. \end{cases} \tag{3}$$

For the above constraint conditions, the optimal engine torque (T_e^*), MG1, and MG2 torque ($T_{\mathrm{MG}i}^*$) can be computed according to the corresponding mode. Taking torque relationship in parallel driving mode as example, the equation is established as follows:

$$\begin{cases} T_e^* = \arg\min[m_{\mathrm{eqv}}(s(t), u(t), t)] \\ T_{\mathrm{MG}i}^* = \arg\min[m_{\mathrm{eqv}}(s(t), u(t), t)] \end{cases} \tag{4}$$

where m_{eqv} is the total equivalent fuel consumption rate, $u(t)$ is the current vehicle speed, $s(t)$ is the current equivalence factor, $T_{\mathrm{e\_max}}$, $T_{\mathrm{MG1\_max}}$, and $T_{\mathrm{MG2\_max}}$ are the maximum output torque of engine, MG1 and MG2, respectively, $\omega_{\mathrm{e\_max}}$, $\omega_{\mathrm{MG1\_max}}$, and $\omega_{\mathrm{MG2\_max}}$ are the maximum speed of engine, MG1 and MG2, respectively, $T_{\mathrm{e\_min}}$, $T_{\mathrm{MG1\_min}}$, and $T_{\mathrm{MG2\_min}}$ are the minimum output torque of engine, MG1 and MG2, respectively, $\omega_{\mathrm{e\_min}}$, $\omega_{\mathrm{MG1\_min}}$, and $\omega_{\mathrm{MG2\_min}}$ are the maximum speed of engine, MG1 and MG2, respectively, $P_{\mathrm{bat\_max}}$ and $P_{\mathrm{bat\_min}}$ are the maximum and minimum battery power, respectively, $\mathrm{SOC}_{\max}$ and $\mathrm{SOC}_{\min}$ are the maximum and minimum battery SOC, respectively, and $I_{\mathrm{bat\_max}}$ and $I_{\mathrm{bat\_min}}$ are the maximum and minimum battery current, respectively.

The control variables change with the working modes. Therefore, it is significant to formulate ECMS with appropriate mode shift rule. According to the minimum shift rule graph of working mode determined in Fig. 10, eight major working modes are required. Among them, there are three pure electric modes and three regenerative braking modes, which form 49 mode shift rules. In fact, not all the mode shift rules are reasonable. As we know, the conventional automatic transmission commonly adopts two clutches to shift but never uses more than two clutches due to complexity. So the state of more than two mode switching elements cannot be changed at the same time during working mode switching. Obviously, the mode shift rules that do not meet the above constrain condition should be deleted. The generation screening process of 49 mode shift rules is illustrated in Fig. 13.

The black solid line indicates that the two working modes can be directly switched. And, the blue dotted line shows that the two connected working modes cannot be switched. While the green dotted line means that the working mode with at least one end cannot be switched in any mode. Based on these rules, the effectiveness of each mode shift rule in Fig. 13 is carefully analyzed. And, only Fig. 13(17) is proved to be valid. So, it can be adopted as the mode shift rule for HEV control strategy.

B. *Feasibility Analysis of FE and Mode Shift Rule*

After screening mode shift rule, the Federal Test Procedure (FTP75) and New European Driving Cycle (NEDC) are adopted to evaluate FE. For the tree (8) in Fig. 11(h), the fuel consumption, battery state of charge (SOC), and operating points of engine, EM1, and EM2 are modeled and simulated. As shown in Fig. 14, the change curves of vehicle speed, acceleration,

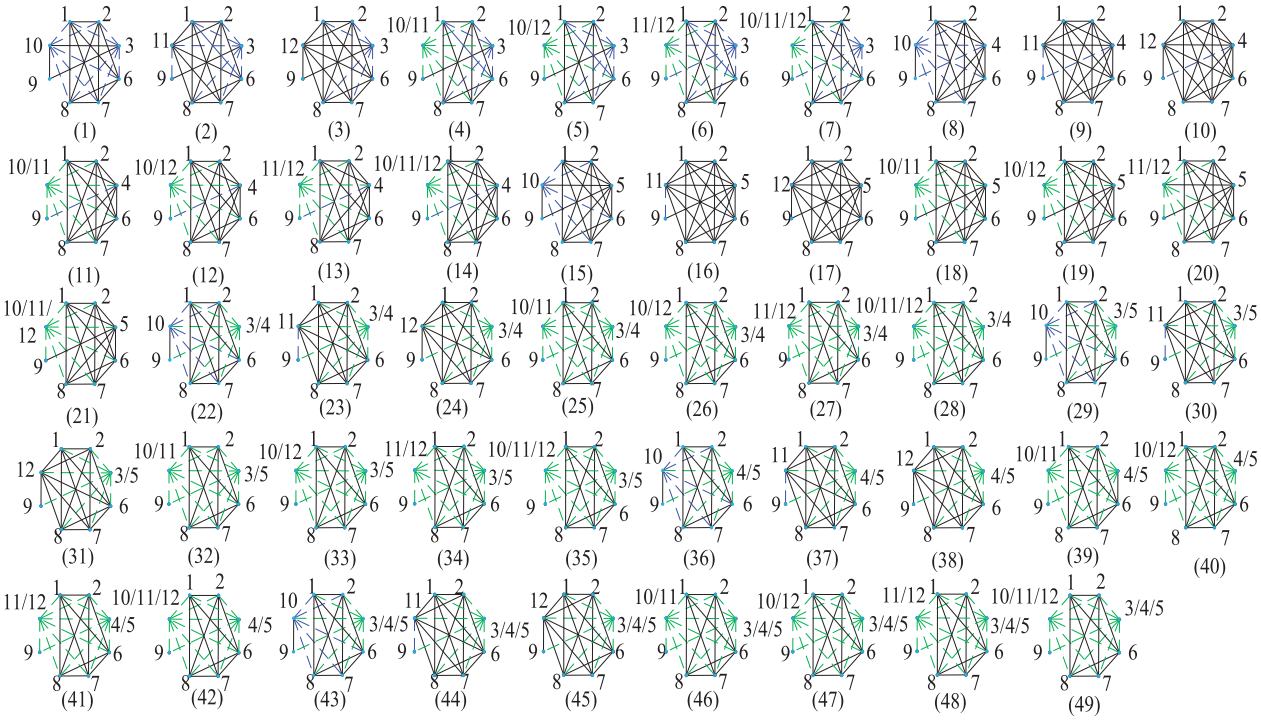

Fig. 13. Generation screening process of 49 mode shift rules.

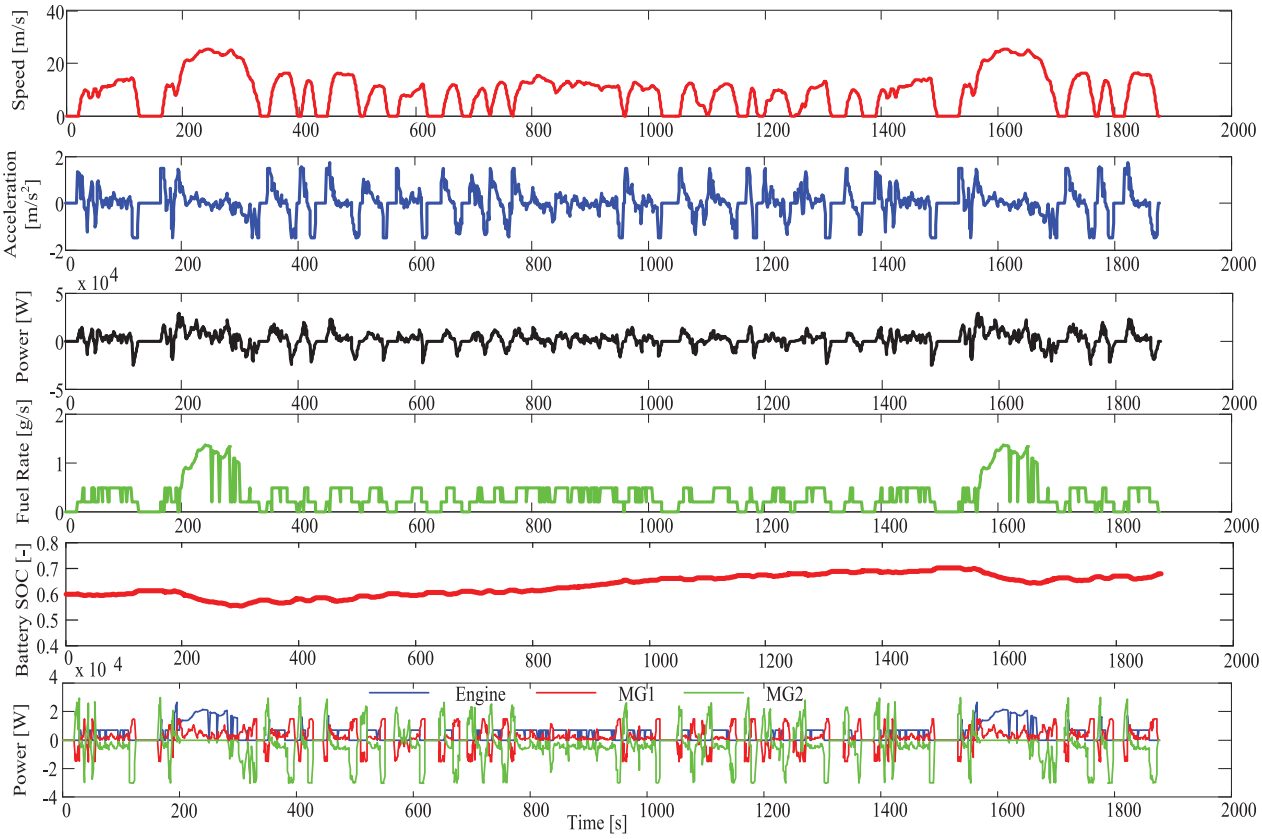

Fig. 14. Simulation results for the multimode configuration: Vehicle speed, acceleration, vehicle power, fuel rate profile, battery SOC, and the actual power (engine, EM1, and EM2) under FTP75.

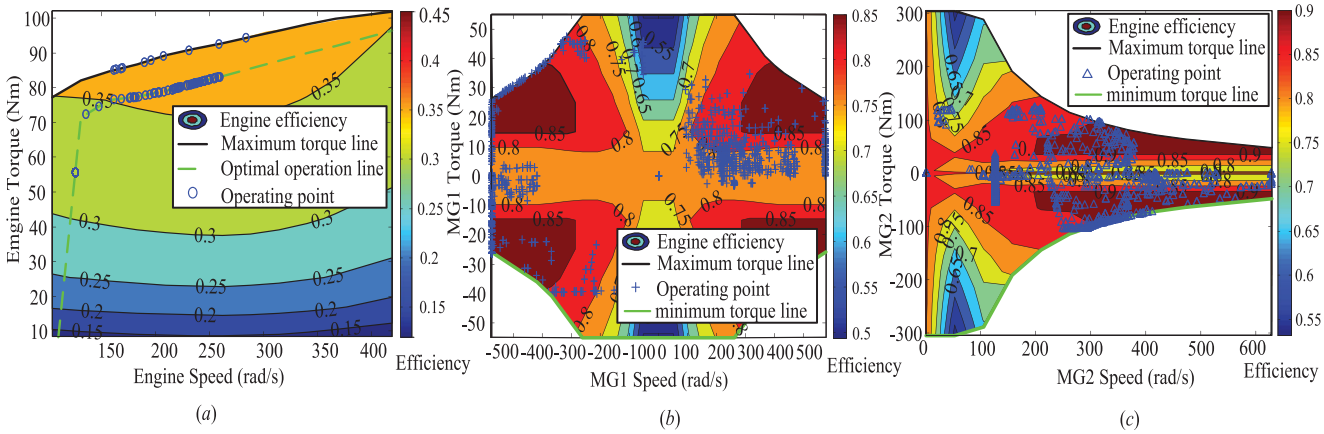

Fig. 15. Distribution of the operation points of multimode configuration under FTP75.

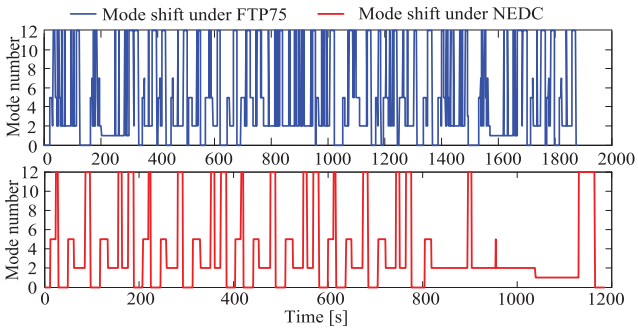

Fig. 16. Mode shift profile for the multimode HEV under FTP75 and NEDC cycle.

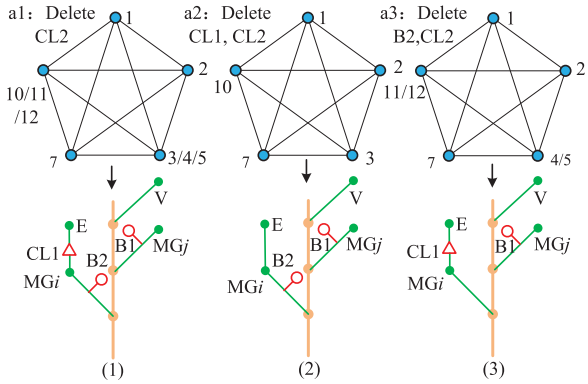

Fig. 17. Three types of new trees.

demand power, fuel rate, battery SOC, and the power profile of engine, EM1, and EM2 for the multimode HEV under FTP75 cycle are presented. Unfortunately, the fuel consumption is 4.94 L/100 km, which is slightly higher than that of the other single mode HEV. This may be because engine, MG1 and MG2 do not all run within high efficiency area. The operating point distributions of engine, MG1, and MG2 are illustrated in Fig. 15. Obviously, engine and MG2 can mostly operate within high efficiency area, while only a few operation points of MG1 are concentrated in high efficiency region, which leads to lower fuel-electricity conversion efficiency. Therefore, the tree (8) needs to be further optimized.

VI. Tree Optimization

Due to speed and torque limit of engine, MG1, and MG2, their working state is not consistent under each mode. Thus, the mode shift rule of multimode HEV needs to be further modified. The actual mode shift profile under FTP75 and NEDC cycle is shown in Fig. 16.

It can be seen that only working mode "1," "2," "5," "7," and "12" are actually in operation. Therefore, the minimum shift rule graph of working mode can be modified. And, three types of trees that meet the requirements can be obtained, as shown in Fig. 17, by repeating the effective tree discrimination process with different numbers of clutches and brakes in Fig. 10.

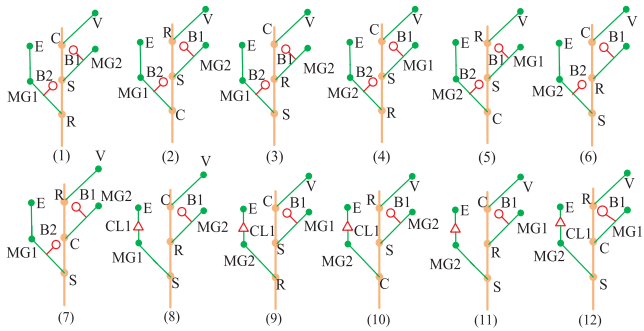

Fig. 18. Twelve feasible trees.

Actually, the actual mode shift profile of trees (1) and (3) in Fig. 17 under FTP 75 cycle is the same as that in Fig. 18. Thus, trees (1) and (3) have the same working mode types, namely working modes "1," "2," "5," "7," and "12." Because the clutches of tree (3) is less than that of tree (1), 24 possible trees need to be analyzed without preliminary screening. Thus, the tree screening method in Section IV is adopted to analyze each major working mode. Among them in Fig. 11, trees (2), (4), (5), and (8) satisfy the power-split mode. And, trees (2), (4), (5), (6), and (8) and (5), (8), (10), (11), and (12) meet EV1 and EV2 mode, respectively. While the trees (2), (4), (5), (8), (10), (11), and (12) meet the parallel driving mode. According to the

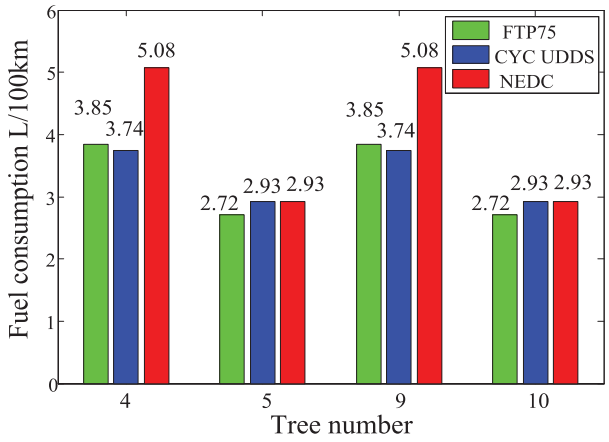

Fig. 19. Comparison of fuel consumption under different cycles.

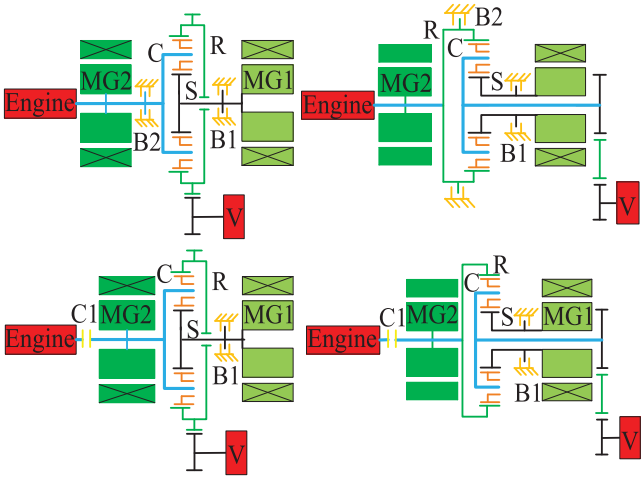

Fig. 20. Four new configurations of multimode HEV.

analysis of working mode, 12 feasible trees can be obtained, as demonstrated in Fig. 18.

To verify the requirements of torque and speed adopted with the mode shift rule for these two types of trees, the analysis process in Section V is carried out. And, only trees (4), (5), (9), and (10) meet the requirements. The fuel consumption of the above four trees is simulated under NEDC, Urban Dynamometer Driving Schedule, and FTP75, respectively, as shown in Fig. 19.

It can be seen that the FE of trees (5) and (10) are significantly better than that of trees (4) and (9). Compared with original tree (8) in Fig. 11, the fuel consumption of trees (4), (5), (9), and (10) decrease by 22.1%, 44.9%, 22.1%, and 44.9% under FTP75 cycle, respectively. This proved the effectiveness of the above optimization process. Hence, there are four new optimal configurations of multimode HEV powertrain, as illustrated in Fig. 20.

VII. Conclusion

A systematic design and optimization method is proposed for multimode HEVs with a single PG, which includes automatic generation of all configurations, formulation of mode shift rules, and configuration screening and optimization. And, a thorough evaluation process for all possible hybrid powertrain with four power sources is presented to verify the effectiveness of this method.

Moreover, an equivalent tree graph is developed to better describe and design new configuration of HEV powertrains. As a result, 48 single-mode and 2304 multimode configurations are obtained. Considering the constraints of requirements of both speed and torque corresponding to main working mode and minimum shift rule graph, one type of the above proposed multimode configurations is explored and screened in detail. Furthermore, the model of multimode HEV is built based on equivalent tree. And the ECMS control strategy is proposed to evaluate FE of optimized configuration, which considers the mode shift rule and optimizes dynamic performance by analyzing the efficiency maps of engine and two motors.

The fuel consumption under FTP75 and NEDC cycles is a little higher than that of the other single mode HEV, which indicates that the FE potential can be further explored. Through screening out the redundant working modes, the minimum shift rule graph is further modified and the novel schemes are developed. Moreover, the FE of optimized configurations under FTP75 cycle is improved by 22.1%–44.9%. It can be concluded that the proposed method is effective to design fuel-efficient powertrain. And, it also reveals that the appropriate mode shift rule and right position and number of clutches and brakes can enhance FE of multimode HEV.

References

[1] F. Hassan, "Plug-in hybrid electric vehicles: Replacing internal combustion engine with clean and renewable energy based auxiliary power sources," *IEEE Trans. Power Electron.*, vol. 33, no. 11, pp. 9611–9618, Nov. 2018.

[2] X. Lu, Y. Qu, Y. Wang, C. Qin, and G. Liu, "A comprehensive review on hybrid power system for PEMFC-HEV: Issues and strategies," *Energy Convers. Manage.*, vol. 171, pp. 1273–1291, 2018.

[3] X. H, Y. Li, C. Lv, and Y. Liu, "Optimal energy management and sizing of a dual motor-driven electric powertrain," *IEEE Trans. Power Electron.*, vol. 34, no. 8, pp. 7489–7501, Aug. 2019.

[4] Y. Cai, M. G. Ouyang, and F. Yang, "Impact of power split configurations on fuel consumption and battery degradation in plug-in hybrid electric city buses," *Appl. Energy*, vol. 188, pp. 257–269, 2017.

[5] P. Zhang, F. Yan, and C. Du, "A comprehensive analysis of energy management strategies for hybrid electric vehicles based on bibliometrics," *Renew. Sustain. Energy Rev.*, vol. 48, pp. 88–104, 2015.

[6] J. Hu, G. Zu, M. Jia, and X. Niu, "Parameter matching and optimal energy management for a novel dual-motor multimodes powertrain system," *Mech. Syst. Signal Process.*, vol. 116, pp. 113–128, 2019.

[7] L. H. Harry, "A comparative study of the production applications of hybrid electric powertrains," *SAE Tech. Paper*, no. 1, pp. 7–23, 2003, Paper 2003-01-2307.

[8] J. M. Miller, "Hybrid electric vehicle propulsion system architectures of the e-CVT type," *IEEE Trans. Power Electron.*, vol. 21, no. 3, pp. 756–767, May 2006.

[9] C. Mansour and D. Clodic, "Dynamic modeling of the electro-mechanical configuration of the Toyota hybrid system series/parallel power train," *Int. J. Automotive Tech.*, vol. 13, no. 1, pp. 143−166, 2012.

[10] T. Barhoumi and D. Kum, "Automatic enumeration of feasible kinematic diagrams for split hybrid configurations with a single planetary gear," *J. Mech. Design*, vol. 139, no. 8, 2017, Art. no. 083301.

[11] F. Zhang, F. Yang, D. Xue, and Y. Cai, "Optimization of compound power split configurations in PHEV bus for fuel consumption and battery degradation decreasing," *Energy*, vol. 169, pp. 937–957, 2019.

[12] X. Zhang, S. Li, H. Peng, and J. Sun, "Design of multimode power-split hybrid vehicles—A case study on the Voltec powertrain system," *IEEE Trans. Veh. Technol.*, vol. 65, no. 6, pp. 4790–4801, Feb. 2016.
[13] W. Zhuang, X. Zhang, D. Li, L. Wang, and G. Yin, "Mode shift map design and integrated energy management control of a multimode hybrid electric vehicle," *Appl. Energy*, vol. 204, pp. 476–488, 2017.
[14] F. Zhu, L. Chen, and C. Yin, "Design and analysis of a novel multimode transmission for a HEV using a single electric machine," *IEEE Trans. Veh. Technol.*, vol. 62, no. 3, pp. 1097–1110, Mar. 2013.
[15] H. L. Benford and M. B. Leising, "The lever analogy: A new tool in transmission analysis," *SAE Tech. Paper*, pp. 429–437, 1981, Paper 810102.
[16] J. Deur, M. Milutinovic, V. Ivanovic, and E. Tseng, "Modeling of a dry dual clutch utilizing a lever-based electromechanical actuator," *J. Dyn. Syst. Meas. Control*, vol. 138, no. 091012, pp. 1–11, 2016.
[17] J. A. Gonzalez and C. Sueur, "Unknown input observer with stability: A structural analysis approach in bond graph," *Eur. J. Control*, vol. 41, pp. 25–43, 2018.
[18] J. Liu and H. Peng, "A systematic design approach for two planetary gear split hybrid vehicles," *Veh. Syst. Dyn.*, vol. 48, no. 11, pp. 1395–1412, 2010.
[19] H. Kim and D. Kum, "Comprehensive design methodology of input- and output-split hybrid electric vehicles: In search of optimal configuration," *IEEE/ASME Trans. Mechatron.*, vol. 21, no. 6, pp. 2912–2923, Dec. 2016.
[20] W. H. Wang, R. F. Song, M. C. Guo, and S. Liu, "Analysis on compound-split configuration of power-split hybrid electric vehicle," *Mech. Mach. Theory*, vol. 78, no. 8, pp. 272–288, 2014.
[21] H. Pei, X. Hu, Y. Yang, X. Tang, C. Hou, and D. Cao, "Configuration optimization for improving fuel efficiency of power split hybrid powertrains with a single planetary gear," *Appl. Energy*, vol. 214, pp. 103–116, 2018.
[22] X. Zhang, C. Li, D. Kum, and H. Peng, "Prius(+) and Volt(-): Configuration analysis of power-split hybrid vehicles with a single planetary gear," *IEEE Trans. Veh. Technol.*, vol. 61, pp. 3544–3552, Oct. 2012.
[23] W. Zhuang, X. Zhang, H. Peng, and L. Wang, "Rapid configuration design of multiple-planetary-gear power-split hybrid powertrain via mode combination," *IEEE/ASME Trans. Mechatron*., vol. 21, pp. 2924–2934, Dec. 2016.
[24] W. Zhuang, X. Zhang, Y. Ding, L. Wang, and X. Hu, "Comparison of multimode hybrid powertrains with multiple planetary gears," *Appl. Energy*, vol. 178, pp. 624–632, 2016.
[25] X. Zhou, D. Qin, and J. Hu, "Multi-objective optimization design and performance evaluation for plug-in hybrid electric vehicle powertrains," *Appl. Energy*, vol. 208, no. 15, pp. 1608–1625, 2017.
[26] J. Yamaguchi, "Toyota readies gasoline/electric hybrid system," *Automotive Eng.*, vol. 105, no. 7, pp. 55–57, 1997.
[27] M. Ehsani, Y. Gao, and J. M. Miller, "Hybrid electric vehicle: Architecture and motor drives," *Proc. IEEE*, vol. 95, no. 4, pp. 719–728, May 2007.
[28] A. Chasse, A. Sciarretta, and J. Chauvin, "Online optimal control of a parallel hybrid with costate adaptation rule," *IFAC Proc.*, vol. 43, pp. 99–104, 2010.
[29] J. Wang, Q. Wang, and P. Wang, "The development and verification of a novel ECMS of hybrid electric bus," *Math. Probl. Eng.*, vol. 6, pp. 331–350, 2014.

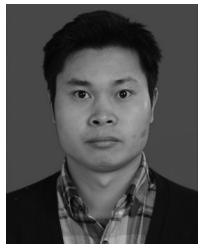

Tao Deng was born in Jiangxi, China, in 1982. He received the Ph.D. degree in vehicle engineering from Chongqing University, Chongqing, China, in 2010.

He is currently a Full Professor with the School of Aeronautics and School of Mechatronics and Vehicle Engineering, Chongqing Jiaotong University, Chongqing, China. His current research interests include power electronic and new energy vehicle theory, design method, and control strategy.

Peng Tang was born in Hubei, China, in 1994. He received the B.S. degree in vehicle engineering in 2017 from Chongqing Jiaotong University, Chongqing, China, where he is currently working toward the M.S. degree in vehicle engineering.

His current research interests include power electronic and new energy vehicle design theory, optimal method, and control strategy.

Zhenghua Su was born in Hunan, China, in 1995. He received the B.S. degree in vehicle engineering in 2017 from Chongqing Jiaotong University, Chongqing, China, where he is currently working toward the M.S. degree in vehicle engineering.

His research interests include multi-DOF motor design and control and new energy vehicle theory.

Yuanping Luo was born in Hunan, China, in 1994. He received the B.S. degree in vehicle engineering in 2017 from Chongqing Jiaotong University, Chongqing, China, where he is currently working toward the M.S. degree in vehicle engineering at Chongqing Jiaotong University, Chongqing, China.

His research interests include new energy vehicles theory and energy management strategy.